Analysis of the NMR Spin−Spin Coupling Mechanism Across a H−Bond: Nature of the H-Bond in Proteins

Tell Tuttle, Jürgen Gräfenstein, Anan Wu, Elfi Kraka, and Dieter Cremer*

Department of Theoretical Chemistry, Göteborg University, Reutersgatan 2, S-413 20 Göteborg, Sweden

Received: August 12, 2003; In Final Form: November 10, 2003

The NMR spin−spin coupling constants (SSCCs) across the H-bond in proteins are sensitive to the electronic structure of the H-bonded system, i.e., the N−H···O═C group in proteins. The spin−spin coupling mechanism across the H-bond involves a strong electric field effect, steric exchange interactions, and some weak covalent effects (transfer of electronic charge). The electric field effect is reflected by one-orbital contributions to the SSCC and can be tested with the help of probe charges. A negative charge opposite to the N−H bond leads to increased polarization of the N−H bond, a larger contact density at the N nucleus, and a stronger FC coupling mechanism for those SSCCs involving the N nucleus. Similarly, a positive charge opposite to the O═C bond, distorts the O density into the direction of the external charge and in this way decreases the spin density at the O nucleus. All SSCCs across the H-bond depend primarily on the electric field effect and two-orbital steric exchange interactions. The lone pair contributions to the Fermi contact term of ^{2h}J(ON) (and to a lesser extent ^{3h}J(CN)) provide a direct measure on possible covalent contributions in the form of charge-transfer interactions. According to calculated charge-transfer values and lone-pair contributions to SSCC ^{2h}J(ON), the covalent contribution to the H-bond is rather small (less than 15% at 1.9 Å for a bending angle β(COH) of 120°). The zeroth-order density and the spin−spin coupling mechanism, which depends largely on the first-order spin density, both describe the H-bond as being electrostatic rather than covalent. The electric field effect largely determines the geometrical dependence of the SSCCs of a hydrogen-bonded system.

1. Introduction

H-bonding is an essential structural building block for many biochemical compounds. Protein folding, molecular recognition, drug−receptor interactions, solvent−solute interactions, and many other phenomena are intrinsically connected to H-bonding.[1−8] For a long time, direct measurements of the H-bond (HB) were difficult, in particular, the low scattering cross-section of the hydrogen atom makes its detection with X-ray diffraction methods a difficult enterprise. Therefore, NMR methods making a site-resolved study of the HB possible represent a valuable source of information, which has the advantage of probing it in the solution phase rather than the solid state as, e.g., neutron diffraction, does.

The experimental observation of spin−spin coupling constants (SSCCs) across the HB, $^{n,h}J$,[9,12] has changed the situation significantly, insofar as for the first time a direct detection of H-bonding in proteins or DNA is possible. This discovery in connection with the intensified discussion of weak HBs[4−8] has triggered a multitude of NMR spectroscopic[9−17] and quantum chemical studies[17−27] on the nature of the HB. The observation of SSCCs across HBs was considered as evidence for a partial covalent nature of the HB.[12,14,20] This interpretation was in line with the covalent character invoked for the low barrier HBs, which are postulated as transition states in several enzyme catalytic reactions.[28−31] The (partial) covalent character was questioned or rejected by others who connected energy or density data with the analysis of SSCCs across the HB.[21]

Here, we will focus on an orbital analysis of the SSCCs of a HB system continuing work recently started with the development of the J-**OC**-PSP method (decomposition of *J* into *O*rbital *C*ontributions using *O*rbital *C*urrents and *P*artial *S*pin *P*olarization).[32−34] J-**OC**-PSP decomposes all four Ramsey terms of the SSCC (paramagnetic spin−orbit (PSO), diamagnetic spin orbit (DSO), Fermi contact (FC), spin dipole (SD))[35] calculated with a coupled perturbed density functional theory (CP-DFT)[36] into one-orbital and two-orbital contributions where, as a suitable choice for the orbitals, Boys localized molecular orbitals (LMOs)[37] are used. The individual orbital terms make it possible to relate the FC and the SD term to a spin polarization mechanism whereas the DSO and PSO orbital terms are associated with orbital currents caused by the magnetic moments of the nuclei. Using the orbital contributions calculated for the SSCCs of small molecules, we could show that the bond orbital contribution of the one-bond SSCC dominates and leads to a positive SSCC, the magnitude of which depends on both the polarity of the bond and the polarizability of the bond density.[33] External bonds (henceforth called *other bonds*[33]) connecting substituents to the bond in question lead to negative contributions because they extend the one-bond path formally to a two-bond path (for unstrained hydrocarbons, a coupling path formed by two σ bond orbitals leads to a negative contribution to the SSCC). In the case of heteroatoms an electron lone pair (lp) also leads to such a "two-bond path" for the one-bond SSCC and consequently to a relatively large negative lp contribution of the FC term. In this way, lp contributions can make a one-bond SSCC negative.[33] Three-bond SSCCs are normally positive, but again substituent contributions can lead to a change in sign.

The orbital analysis of the SSCCs across HBs provides a basis to determine those contributions, which determine the magnitude and the sign of a given SSCC. In addition, it is possible to identify orbital terms that indicate covalent and those that stand for an electrostatic nature of the HB. Furthermore, we can

10.1021/jp0363951 CCC: $27.50
Published on Web 12/24/2003

SCHEME 1

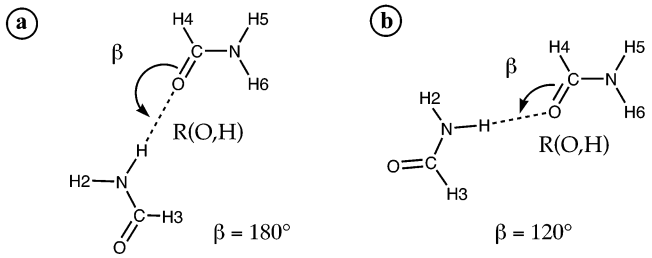

distinguish active and passive contributions of an orbital to the spin−spin coupling mechanism. In the case of the FC term, an active contribution implies that the orbital in question determines directly the spin density at the coupling nuclei whereas a passive contribution mediates spin-polarization between two orbitals, each of which determines the spin density just on one of the coupling nuclei. Utilizing the possibilities of the orbital analysis, the relationship between the SSCC and the nature of the HB will become clear. For the purpose of testing the usefulness of such an analysis, we will investigate a typical HB as it occurs in polypeptides and proteins and as it can be modeled by the formamide dimer, namely, the HB C═O···H−N (see Scheme 1). We will analyze the six SSCCs directly, or indirectly, affected by H-bonding for two typical geometrical situations: first a linear arrangement of C═O and H−N bond given by the angle $\beta = 180°$ (Scheme 1) and second a bent arrangement given by $\beta = 120°$ (Scheme 1). The angle α(NHO) is kept constant at 169.6° as it has a smaller effect on the SSCC across the H-bond. Furthermore, the two dimers are kept in a common plane to simplify the analysis.

We will carry out the analysis of SSCCs across the HB in the following way: First we will use a model system made up of two H_2 molecules to understand how interactions between separated molecules can influence through-space SSCCs (section 3). In this system, HB interactions do not play any role. Therefore, we can study the influences of symmetry and topology as well as the general impact of nonbonded effects on the SSCC. We will show that electric field and steric exchange effects are responsible for through-space SSCCs and with this knowledge we will analyze the HB C═O···H−N (section 4). However, we will start by first giving some relevant details on the calculational methods used in this work.

2. Decomposition of the Spin−Spin Coupling Constant into Orbital Contributions

The two model systems investigated in this work were defined in the following way. In the case of the $(H_2)_2$ dimer the experimental equilibrium geometry of H_2 (R(H1,H2) = 0.741 Å[38]) was used and the two molecules were arranged linearly by varying the nonbonded distance R(H2,H3) between 1.0 and 5.0 Å. For the formamide dimer, a planar arrangement (shown in Scheme 1) with a single HB rather than two HBs was assumed to model H-bonding in proteins. The geometry for this arrangement was calculated by employing second-order many body perturbation theory with the Møller−Plesset perturbation operator (MBPT2)[39] and using Dunning's aug-cc-pVDZ basis set.[40] In the equilibrium geometry of the formamide dimer (see Figure 1a), the molecular planes enclose an angle χ of −78.5°. For the purpose of simplifying the SSCC analysis, χ was reduced to zero so that the two formamide molecules are in a common plane. The complex binding energy (after basis set superposition error corrections) decreases from its equilibrium value of 5.8 kcal/mol by 1.5 to 4.3 kcal/mol and the geometrical parameters

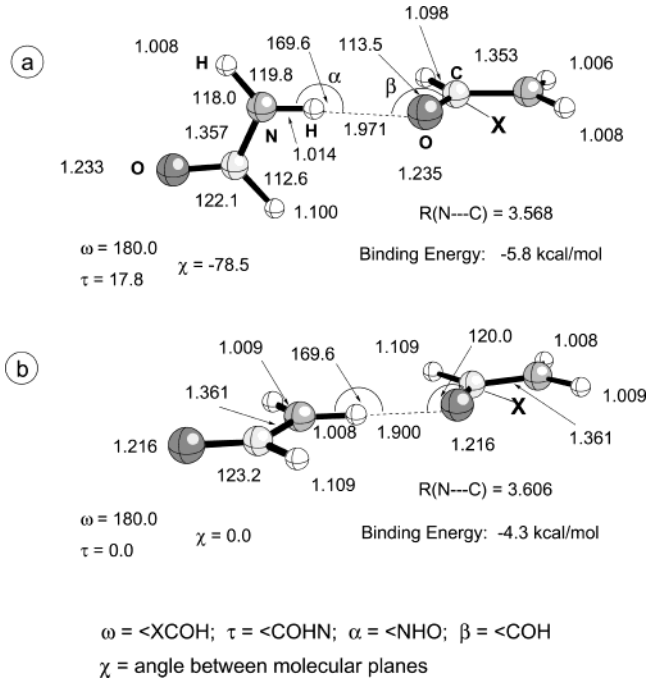

Figure 1. MBPT2/aug-cc-pVDZ geometries and binding energies for the formamide dimer: (a) minimum geometry; (b) enforced planarity. Distances in ångstroms; angles in degrees. X is a dummy atom used to define dihedral angles.

change slightly as indicated in Figure 1b. Hence, the model chosen represents one of many possible geometrical arrangements of the HB, which, however, is typical and easy to analyze. The HB geometry is determined by the angles α(NHO) = α and β(COH) = β. Angle α was frozen at its equilibrium value (169.6°) whereas β was set to 180 and 120°. In this way, two principally different HB configurations (linear and bent) were modeled and investigated.

The calculation of the indirect scalar SSCCs J involving the nuclei of the HB system were computed as the sum of the four Ramsey terms[35] (FC, DSO, PSO, SD) that comprise the coupling constant. This was done using the CP-DFT method described by Cremer and co-workers,[36] utilizing the B3LYP functional[41,42] and two basis sets, (9s,5p,1d/5s,1p)[6s,4p,1d/3s,1p] and (11s,7p,2d/5s,1p)[7s,6p,2d/4s,2p],[43] which were developed for the calculation of magnetic properties.

The SSCCs were calculated both as J values expressed in hertz and as reduced SSCCs K expressed in SI units. The relationship between these two quantities is given by $J(A,B) = (h/4\pi)\gamma_A\gamma_B K(A,B)$. The following gyromagnetic ratios (given in units of 10^7rad T^{-1} s^{-1}) were used for nuclei A and B: $\gamma(^1H) = 26.7522$, $\gamma(^{13}C) = 6.7263$, $\gamma(^{15}N) = -2.7126$, and $\gamma(^{17}O) = -3.6266$.[44]

The theory of the J-**OC**-PSP method has been described elsewhere.[32−34] Therefore, we mention just a few pertinent essentials for the present investigation. The localization of the orbitals according to Boys[37] is carried out for core, σ, and π orbitals separately. In this way, long valence tails of the core LMOs, which lead to unrealistic core contributions, and bent bond LMOs, in the case of double bonds, are avoided. The individual orbital contributions depend on both zeroth-order and first-order orbitals (with the exception of the DSO contributions, which depend on just the zeroth-order orbitals). Because the FC term turns out to be the most important for most SSCCs investigated in this work, we will discuss shortly the first-order orbitals and the corresponding first-order spin density associated with the FC term. The first-order (canonical) spin−orbital

(equivalent equations hold for LMOs) is given by

$$\psi_{k\sigma}^{(B),FC} = \sum_{a\sigma'}^{virt} \frac{\langle \psi_{a\sigma'}^{(0)} | \mathbf{F}_A^{FC} | \psi_{k\sigma}^{(0)} \rangle}{\epsilon_k - \epsilon_a} | \psi_{a\sigma'}^{(0)} \rangle \quad (1)$$

where $\psi^{(0)}$ is a zeroth-order spin−orbital, first-order spin−orbital $\psi^{(B),FC}$ is generated by the FC perturbation at nucleus B, and indices k and a denote occupied and virtual (virt) orbitals; σ and σ' are spin variables. The operator $\mathbf{F}_A^{FC}$ is the first-order term of the perturbed Kohn−Sham operator and depends itself on the first-order orbital $\psi_{k\sigma}^{(B),FC}$:

$$\mathbf{F}_A^{FC} = \mathbf{H}_A^{FC} + \tilde{\mathbf{F}}_A^{FC} \quad (2a)$$

$$\tilde{\mathbf{F}}_A^{FC} = \sum_{k\sigma}^{occ} \int d^3r \frac{\partial \mathbf{F}}{\partial \psi_{k\sigma}(\mathbf{r})} \psi_{k\sigma}^{(B),FC}(\mathbf{r}) \quad (2b)$$

The Fermi contact spin density distribution is given by the product of zeroth-order and first-order spin−orbitals summed over all occupied orbitals:

$$\rho^{(B),FC}(\mathbf{r}) = 2 \sum_{k}^{occ} \sum_{\sigma} \psi_{k\sigma}^{(0)}(\mathbf{r}) \psi_{k\sigma}^{(B),FC}(\mathbf{r}) \quad (3)$$

The Fermi contact spin density distribution at the position $\mathbf{R}_A$ of the responding nucleus A determines the FC term of the SSCC:

$$K_{AB}^{FC} = \frac{8}{3} \pi \alpha^2 \rho^{(B),FC}(\mathbf{R}_A) \quad (4)$$

where α is the hyperfine coupling constant. Hence, one can analyze the sign and magnitude of the FC term by investigating the FC density distribution, which itself depends on the various orbital products $\psi_{k\sigma}^{(0)} \psi_{k\sigma}^{(B),FC}$. One can partition the FC spin density distribution into orbital contributions where, however, one must consider eqs 1 and 2; i.e., besides the one-orbital terms $\rho_k^{(B),FC}$ depending only on ψ_k, there are also two-orbital terms $\rho_{k,l}^{(B),FC}$ depending on both $\psi_{k\sigma}^{(0)}$ and $\psi_{l\sigma}^{(B),FC}$. Accordingly, one obtains for the FC part of the SSCC, an equation in terms of FC spin density distributions expressed in zeroth- and first-order orbitals:[33]

$$K_{AB}^{FC} = \frac{8}{3} \pi \alpha^2 [\sum_k \rho_k^{(B),FC}(\mathbf{R}_A) + \sum_k \sum_l \rho_{k,l}^{(B),FC}(\mathbf{R}_A)] \quad (5)$$

where

$$\rho_k^{(B),FC}(\mathbf{r}) = 2 \sum_{\sigma}^{occ} \sum_{a\sigma'}^{virt} \frac{\langle \psi_{a\sigma'}^{(0)} | h_{k,z}^{(B),FC} + \tilde{F}_{k,z}^{(B),FC} | \psi_{k\sigma}^{(0)} \rangle}{\epsilon_k - \epsilon_a} \psi_{a\sigma'}^{(0)}(\mathbf{r}) \, \psi_{k\sigma}^{(0)}(\mathbf{r}) \quad (6a)$$

$$\rho_{kl}^{(B),FC}(\mathbf{r}) = 2 \sum_{\sigma}^{occ} \sum_{a\sigma'}^{virt} \frac{\langle \psi_{a\sigma'}^{(0)} | \tilde{F}_{l,z}^{(B),FC} | \psi_{k\sigma}^{(0)} \rangle}{\epsilon_k - \epsilon_a} \psi_{a\sigma'}^{(0)}(\mathbf{r}) \, \psi_{k\sigma}^{(0)}(\mathbf{r}) \quad (6b)$$

The one-orbital contribution describes orbital relaxation caused by the magnetic perturbation at nucleus B. This can be due to a repolarization of, e.g., a bond density (if bonding LMO k and the excitation $k \rightarrow k^*$ are considered) or due to a delocalization of this bond density into the antibonding LMO l of another bond (excitation $k \rightarrow l^*$). In the case of two interacting molecules, the first contribution results from electrostatic (noncovalent) repulsion or attraction mediated by an electric field generated by each of the molecules. The second contribution will become only important if at closer distance the overlap between the orbitals k (first molecule) and l^* (second molecule) is large enough to guarantee a significant charge transfer and by this covalent interactions. Repolarization (noncovalent) and delocalization (covalent) one-orbital contributions affecting through-space or trans-HB SSCCs can be directly calculated with the J-**OC**-PSP method by resolving in eq 1 the sum over virtual orbitals.[32,33]

The two-orbital contributions describe steric exchange interactions between orbitals k and l.[33] Again, if orbital l belongs to the first molecule (the perturbation is at orbital l) and orbital k to the second (k is the responding orbital), the two-orbital terms can be associated with noncovalent interactions between the molecules. We denote the two-orbital interactions by the symbol $(k \leftarrow l)$ where l is the zeroth-order and k the first-order orbital. The contributions $(k \leftarrow l)$ and $(l \leftarrow k)$ are different, and therefore, both have to be considered. However, for reasons of simplicity we contract them to a contribution $(k, l) = (k \leftarrow l) + (l \leftarrow k)$ and list only the sum of the two contributions. Where necessary, the individual terms are analyzed. The various orbital terms investigated will be denoted by the abbreviations bd (bond orbital contribution) and lp (lone pair orbital contribution) connected with numbers or atom symbols to simplify their identification (bd1, bd2, lp(O), etc.). We will use the symbols σ(AB) and π(AB) to separate the orbital contributions of a double bond.

We distinguish between active and passive orbital contributions where the former are directly calculated as described above. If an orbital does not lead to an active contribution of the spin−spin coupling mechanism, it can still make a contribution in a passive way by mediating spin polarization or orbital currents from an orbital perturbed at one nucleus to another orbital interacting with the nuclear moment of the second nucleus. The passive orbitals lead to the manifold of different coupling paths typical for spin−spin coupling, and therefore, they are essential for the orbital analysis. We calculate the sum of active and passive contribution of a particular orbital by freezing it when determining the SSCC. Subtracting its active contribution leads to the passive contribution.

The FC part of the SSCCs decomposed into orbital contributions reveals whether covalent or noncovalent terms play an important role for the spin−spin transmission mechanism. Although this mechanism depends on the first-order density, it is a fact that the zeroth-order density $\rho^{(0)}$ will not be changed by the spin polarization (first-order density); i.e., changes in the α- and β- spin density distribution cancel each other out. Analysis of the spin−spin coupling mechanism and the first-order density must lead to the same conclusions, with regard to the nature of through-space interactions or H-bonding, as an analysis of the zeroth-order density. Furthermore, the spin−spin coupling mechanism and the first-order density provide much more sensitive antenna to investigate the nature of molecular interactions, making them ideally suited for weak interactions.

We tested basis set superposition errors (BSSE) for the SSCCs of monomers and dimers using the counterpoise method.[45] In the case of the H_2 monomer, the error was just 0.3 Hz, and in the case of the formamide dimer, it did not become larger than 0.8 Hz.

All SSCC calculations were performed with the quantum chemical program package COLOGNE 2003.[46]

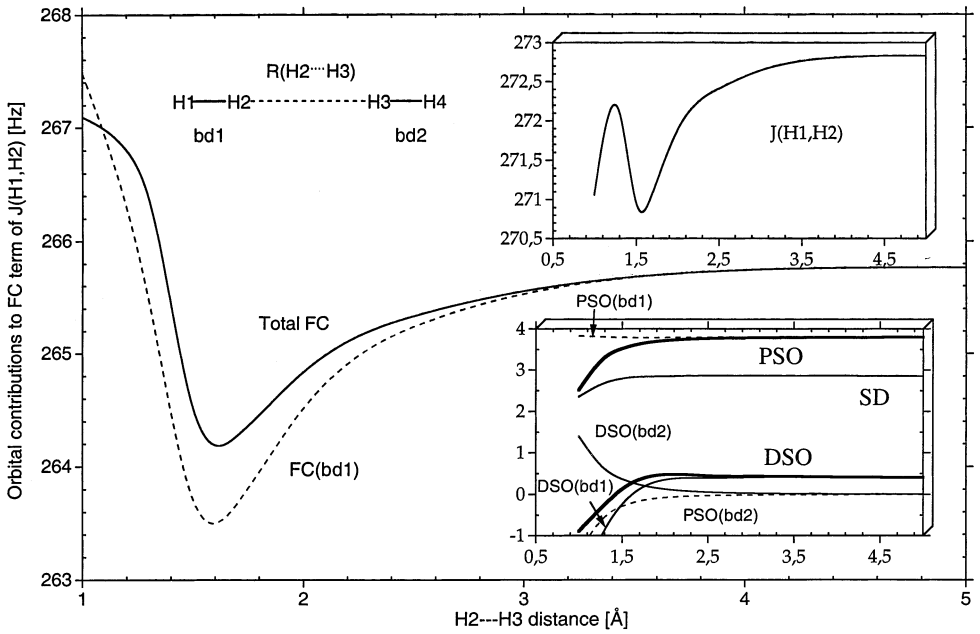

Figure 2. Dependence of the SSCC ^1J(H1,H2) of the H_2 dimer on the distance R(H2,H3). The main diagram gives the total FC term and the dominating one-orbital contribution bd1 (σ(H1,H2)) and the inset at the top displays the total SSCC ^1J(H1,H2). The inset at the bottom shows PSO, DSO, and SD terms as well as the dominating one-orbital contributions to DSO and PSO term. CP-DFT/B3LYP/(11s,7p,2d/5s,1p)[7s,6p,2d/4s,2p] calculations.

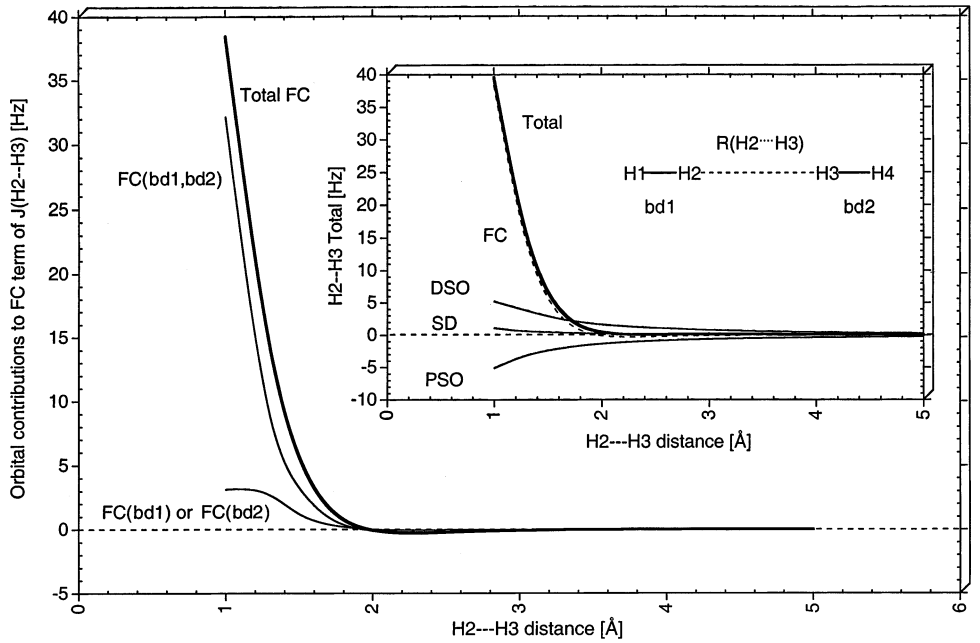

Figure 3. Dependence of the SSCC ^1J(H2,H3) of the H_2 dimer on the distance R(H2,H3). The main diagram gives gives the total FC term and the dominating two- and one-orbital contributions and the inset displays the total SSCC J(H1,H2) and its four Ramsey terms. CP-DFT/B3LYP/(11s,7p,2d/5s,1p)[7s,6p,2d/4s,2p] calculations.

3. Through-Space Spin−Spin Coupling Constants in the H_2 Dimer

The calculated SSCCs ^1J(H1,H2), ^1J(H2,H3), ^2J(H1,H3), and ^3J(H1,H4) for two H_2 molecules interacting at a distance R(H2,H3) in a linear arrangement are summarized in graphical form in Figures 2−5. For H_2 at equilibrium a one-bond SSCC of 272.7 Hz corresponding to ^1J(H,D) = 41.9 Hz is calculated. Adding a vibrational correction of 1.3 Hz,[47] the calculated ^1J(H,D) (43.2 Hz) is close to the experimental ^1J(H,D) value of 42.9 Hz.[47] We conclude that the CP-DFT method[36] used in this work is sufficiently accurate to describe spin−spin coupling in the model system $(H_2)_2$.

The mechanism of the SSCC ^1J(H1,H2) is dominated by the FC interaction involving the bond orbital bd1 = bd1(H1,H2). There are changes in this orbital and the corresponding density as reflected by the DSO contribution. At shorter R(H2,H3), nonbonding density is pushed into the H1−H2 bond by exchange repulsion between the two molecules, thus leading to a negative DSO(bd1) contribution. In previous work, we have shown that those parts of the electron density distribution that are inside the sphere enveloping the bond axis A−B give negative contributions to the DSO term, whereas the electron density outside this sphere leads to positive contributions.[36a] The DSO contribution of bd2 = bd2(H3,H4), which builds up

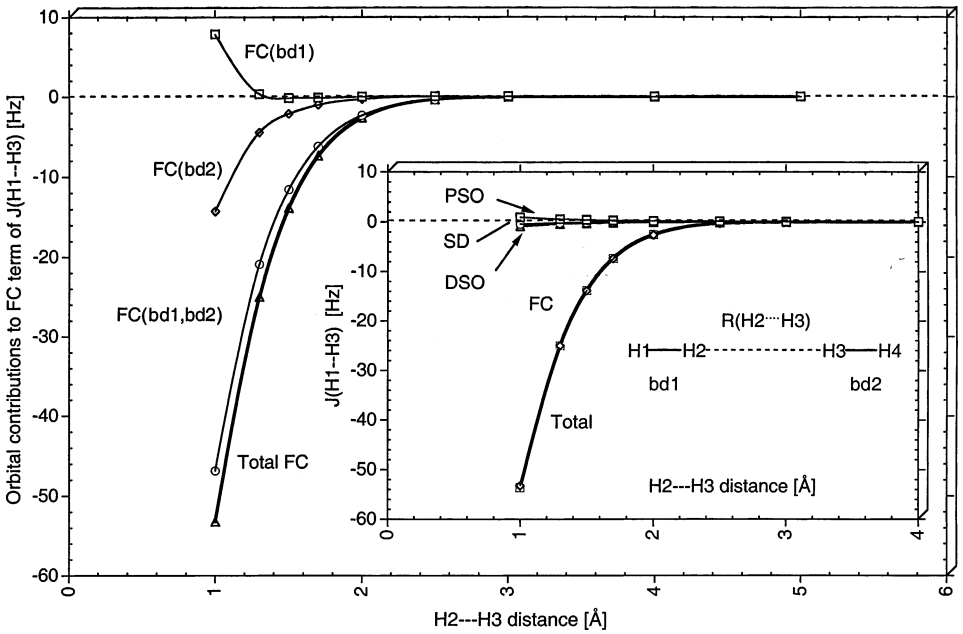

Figure 4. Dependence of the SSCC ^2J(H1,H3) of the H_2 dimer on the distance R(H2,H3). The main diagram gives gives the total FC term and the dominating two- and one-orbital contributions and the inset displays the total SSCC ^2J(H1,H3) and its four Ramsey terms. CP-DFT/B3LYP/(11s,7p,2d/5s,1p)[7s,6p,2d/4s,2p] calculations.

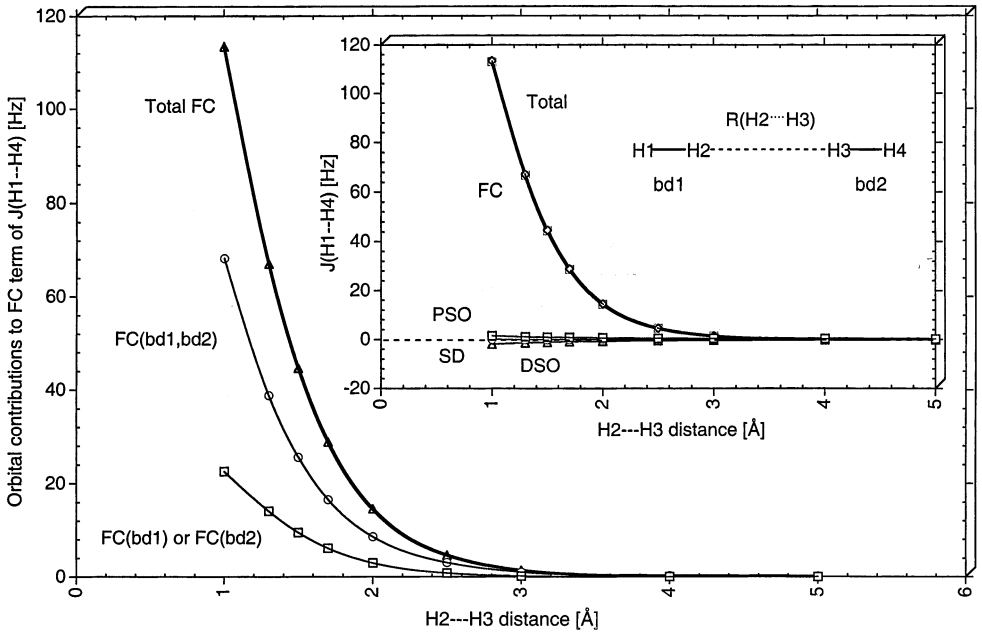

Figure 5. Dependence of the SSCC ^3J(H1,H4) of the H_2 dimer on the distance R(H2,H3). The main diagram gives gives the total FC term and the dominating two- and one-orbital contributions and the inset displays the total SSCC ^3J(H1,H4) and its four Ramsey terms. CP-DFT/B3LYP/(11s,7p,2d/5s,1p)[7s,6p,2d/4s,2p] calculations.

outside the bond H1−H2 for small R(H2,H3) leads to a positive contribution (see inset in Figure 2). The FC term is dominated by FC(bd1) (see Figure 2) and reveals that for decreasing R(H2,H3) the one orbital contribution FC(bd1) decreases. A minimum is reached at 1.6 Å. At smaller values of R(H2,H3) first strong polarizing and finally covalent interactions play a role. The total value of ^1J(H1,H2) increases due to the increase of the FC contribution in this region but then decreases as a reflection of the decrease in both the PSO, DSO, and SD terms (see insets in Figure 2). Because we are primarily interested in the through-space SSCC between the two molecules, it is appropriate to investigate the spin−spin coupling mechanism in the region beyond R(H2,H3) = 1.6 Å as in this region significant covalent interactions can be excluded. Nevertheless, it is also useful to look at distances as short as 1 Å because for these R(H2,H3) values, effects are magnified so that it is easier to make them visible.

The through-space magnetic couplings are mediated by spin polarization in the tail densities of bond orbitals bd1 and bd2 in the nonbonded region between H2 and H3. This should be reflected by the FC term. PSO, DSO, and SD contributions are small in the case of the H_2 dimer. A priori, one could expect that all SSCCs across the nonbonded region are of the same, small magnitude. However, this is not the case: ^1J(H2,H3) < $|^2J$(H1,H3)| < ^3J(H1,H4) at all distances 1.0 < R(H2,H3) < 5 Å (see Figures 3−5). SSCCs ^1J(H2,H3) and ^3J(H1,H4) similar to ^1J(H1,H2) are always positive whereas ^2J(H1,H3) is always negative. In all cases, the FC term dominates the magnitude of

the SSCC, although for ^1J(H1,H2), ^1J(H2,H3), and ^3J(H1,H4) the noncontact terms are nonnegligible. However, mostly they cancel each other out to a large extent (see Figures 2−5).

The orbital analysis reveals that, contrary to the one-bond SSCC ^1J(H1,H2), the two-orbital terms describing steric exchange interactions are responsible for both magnitude and sign of the through-space SSCCs. Steric exchange interactions between the two bonding electron pairs depend on the overlap between the bonding orbitals, which decreases exponentially with increasing distance. Accordingly, the (bd1, bd2) orbital contribution to the FC term, the FC contribution to the total SSCC, and by this the total SSCCs ^1J(H2,H3), $|^2J$(H1,H3)|, and ^3J(H1,H4) all decrease exponentially with increasing distance R(H2,H3) (see Figures 3−5).

The different signs and magnitudes of the three SSCCs are a result of different spin densities at the coupling nuclei as becomes obvious when analyzing zeroth- and first-order LMOs bd1 and bd2 as well as the FC spin density distribution according to eqs 5 and 6. In Figure 6, orbitals and FC spin density distributions are shown in the form of contour line diagrams. Of the two terms contributing to (bd1, bd2), only the one with the larger magnitude is shown. In the case of FC(H2,H3), this is (bd1 ← bd2), in the cases of FC(H1,H3) and FC(H1,H4) (bd2 ← bd1). As a result of the interactions between the two H_2 molecules, the bonding LMOs are distorted toward the second H_2 molecule so that at small R(H2,H3) values, nuclei H1, H2, and H3 (H4, H3; and H2) are all located in the front lobe of LMO bd1 (LMO bd2) whereas only H4 (H1) is in the back lobe of the orbital (see Figure 6a,b). For very large R, the nodal plane of the LMO bd1 is shifted out of the second H_2 molecule into the intermolecular region. However, for the R(H2,H3) distances investigated either H3 or H2 is close to the nodal plane of the zeroth-order LMO.

If the magnetic perturbation is applied at nucleus H2 with regard to zeroth-order LMO bd2, the first-order LMO bd1 (Figure 6b) is obtained, which possesses an additional nodal surface. The amplitudes of zeroth-order LMO bd1 at H1 and H2 are positive whereas the corresponding amplitudes of the first-order LMO are positive and negative (Figure 6b). For ^1J(H2,H3) (or ^1K(H2,H3)), the product of the amplitudes of zeroth-order and first-order orbital at the first nucleus multiplied with the corresponding product of the amplitudes at the second nucleus is proportional to the SSCC. At H2, there is a predominance of β FC spin density (dashed contour lines in Figure 6c; nucleus H2 is perturbed choosing an α spin for this nucleus) and at H3 a predominance of α FC spin density (solid contour lines in Figure 6c). This means that ^1J(H2,H3) must be positive. The calculated Fermi contact spin density is relatively small at H3 (reflected by the number of contour lines surrounding the nucleus), which leads to a small SSCC ^1J(H2,H3) (Figure 6c).

The analysis presented in Figure 6a,b,c can be presented in a Dirac vector model.[32,33] If the perturbed nucleus H2 has α-spin, there is a dominance of β-spin density for the electrons at this nucleus (Fermi coupling). Due to the different positions of the nodal surfaces of zeroth-order and first-order orbital (outside and inside the nonbonded region H2·H3, Figure 6), there is a dominance of α-spin for the electrons at nucleus H3, which adopts β-spin by Fermi coupling. A positive SSCC results (see Scheme 2a). One could interpret this result also in the sense that Pauli coupling leads to a predominance of α spin density at H3; however, Pauli coupling is only valid in the case of strong electron pairing as in a bond and also at larger values of

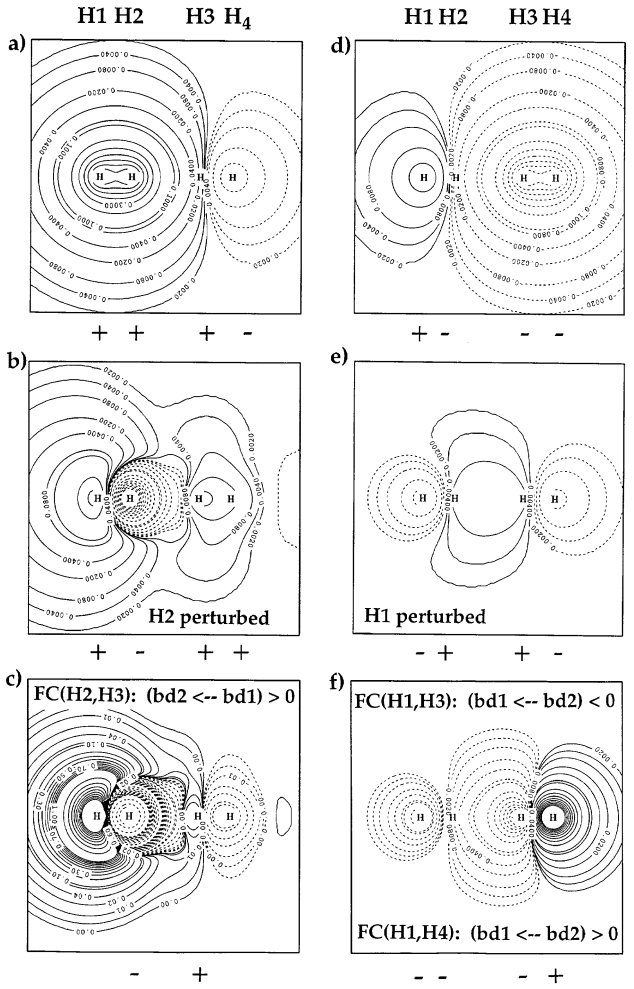

Figure 6. Contour line diagram of (a) the H1−H2 bonding LMO bd1 of the H_2 dimer, (b) the first-order LMO bd2 (perturbation at H2), (c) the FC spin density distribution of the two-orbital term (bd2 ← bd1) of FC(H2,H3) (perturbation at H2), (d) the H3−H4 bonding LMO bd2 of the H_2 dimer, (e) the first-order LMO bd1 (perturbation at H1), and (f) the FC spin density distribution of the two-orbital term (bd1 ← bd2) of FC(H1,H3) and FC(H1,H4) (perturbation at H1). Solid contour lines indicate a positive orbital amplitude (FC spin density distribution, i.e., more α-density), and dashed contour lines a negative orbital amplitude (FC spin density distribution, i.e., more β-density). The signs of the orbital and spin density at the coupling nuclei are given below each diagram. Contour levels are magnified by 100 for clarity in the case of (c) and (f). CP-DFT/B3LYP/(11s,7p,2d/5s,1p)[7s,6p,2d/4s,2p] calculations, with R(H2,H3) = 1.6 Å.

R(H2,H3) the dominating FC spin density at H3 can become β, thus yielding a negative FC(H2,H3) (see Figure 3).

If the perturbation is at H1 (as in the case of ^1J(H1,H2), ^2J(H1,H3), or ^3J(H1,H4)) the steric exchange contribution (larger term) to ^3J(H1,H4) is positive (β FC spin density at H1; α at H4), as can be quickly verified by the signs of zeroth-order and first-order LMO at the coupling nuclei (Figures 6d,e,f). In the case of ^2J(H1,H3), a positive and a negative contribution result (Figure 6f) where the negative is dominant. Accordingly, $|^2J$(H1,H3)| is smaller than the positive ^3J(H1,H4). The results are summarized in the Dirac vector model shown in Scheme 2a, where the perturbation had to be placed at nucleus H4 rather than H1 to display all coupling situations in one diagram. However, H1 and H4 are equivalent nuclei.

The different magnitudes of the through-space SSCCs are a result of the steric exchange interactions between the two H_2 molecules, which lead to distorted zeroth-order LMOs. For decreasing R(H2,H3), the nodal surface of the zeroth-order LMO

SCHEME 2

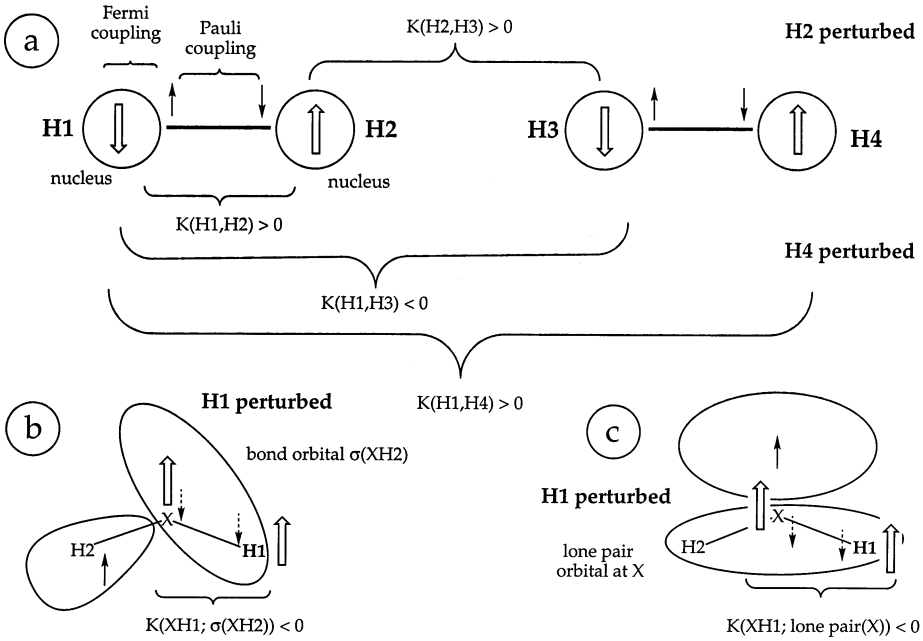

bd1 moves toward molecule H3H4, through the position of nucleus H3 and into the bond region of H3−H4. The sign of bd1 changes from minus to plus whereas the first-order LMO bd2 essentially keeps its form. Accordingly the FC term of SSCC ^1J(H2,H3) is first slightly negative (Figure 2), becomes zero at 2 Å, and increases to large, positive values as the nonbonded interactions are replaced by covalent interactions. Hence, ^1J(H2,H3) depends on the distance R(H2,H3), which determines the topology of the nodal surfaces. The latter implies that either at H2 or H3, the spin density is rather small. This can be avoided for ^2J(H1,H3), but now the topology of the nodal planes implies that one steric exchange contribution is negative and the other positive where the negative term dominates. For ^3J(H1,H4), the spin densities at the nuclei are relatively large because the nodal surfaces of LMOs bd1 and bd2 are always separated from these nuclei.

We note in this connection that one has to distinguish between atomic densities, s-densities at the nuclei, and the spin densities at the nuclei. Only the latter determine the magnitude and the sign of the FC term, the atomic densities are irrelevant in this respect. The s-densities are often used to estimate the magnitude of the FC term; however, one has to realize that a large s-density of the zeroth-order LMO does not necessarily imply a large spin density. For example, steric exchange pushes the density out of the intermolecular region on to the nuclei H2 and H3, then into the bond regions, and finally onto H1 and H4. Consequently, the atomic densities of H2 and H3 are slightly smaller than those of H1 and H4 whereas the s-densities at nuclei H2 and H3 are larger than those at nuclei H1 and H4. These are zeroth-order effects, which are only relevant for the DSO term. The spin density distribution is no longer symmetric because it depends on the position of the perturbed nucleus. If H2 is perturbed, there is large spin polarization in the bond H1−H2 and at H1 (leading to a large ^1J(H1,H2)), however, only little spin polarization at H3 and H4. Consequently, ^1J(H2,H3) is small.

It is noteworthy that ^1J(H2,H3), although small, has sizable PSO and DSO contributions of opposite sign (at $R = 2$ Å: PSO, −2 Hz; DSO, 0.8 Hz), which cancel each other partially. The sign of the DSO term must be positive because most of the relevant density is outside the nonbonded region H2−H3 (for a detailed explanation, see refs 34 and 36a). The PSO term results from the fact that the first-order LMOs adopt pσ−pσ character. Considering that the gradient of the first-order orbital enters the PSO term, a negative contribution must result.

In conclusion, orbital symmetry and topology depending on the actual distance R(H2,H3) determines the relative magnitude of the through-space SSCCs in the H_2 dimer. We will see in section 4 whether this also applies to the SSCCs across a H-bond.

4. Spin−Spin Coupling Across the H-Bond

H-bonding in proteins involves, in most cases, arrangements of the type C═O···H−N, which can be modeled by the formamide dimer (which, of course, does not consider cooperative effects between different parts of a protein). Six SSCCs should be affected by H-bonding, four directly because they are across the HB SSCCs and two indirectly because they involve atoms participating in H-bonding. Numbering atoms in analogy to the (H_2·H_2) complex, there is the 1,4-SSCC ^{3h}J(CN), the two 1,3-SSCCs ^{2h}J(CH) and ^{2h}J(ON), and finally the 2,3-SSCC ^{1h}J(OH). Two of them, namely, ^{3h}J(CN) and ^{2h}J(CH), should be measurable whereas the other two, namely, ^{2h}J(ON) and ^{1h}J(OH), are difficult to measure because of the large line width of the ^{17}O signal, due to the quadrupolar relaxation mechanism for ^{17}O. The nuclear spin of ^{17}O is $^5/_2$, which implies that each spin coupled to ^{17}O leads to a six-line pattern, thus yielding for smaller SSCCs just very broad lines.[48] The one-bond SSCCs ^1J(NH) and ^1J(CO) are indirectly affected by H-bonding and there is a chance that changes in their magnitude can be used to describe H-bonding. ^1J(NH) is routinely measured[49] whereas ^1J(CO) is seldom measured[50] for the same reasons as the other SSCCs involving ^{17}O. We will discuss here all six SSCCs directly or indirectly affected by H-bonding considering the following questions:

(1) How does spin−spin coupling change relative to the (H_2·H_2) complex considering the sign and magnitude of the SSCCs?

(2) What is the mechanism for spin−spin coupling across the HB? Which orbitals are involved? Are one- or two-orbital terms dominant? What is the role of the lone-pair orbitals?

(3) How do the SSCCs depend on the nature of H-bonding?

TABLE 1: Decomposition of the NMR Spin−Spin Coupling Constants Across and at the Hydrogen Bond in the Formamide Dimer into Orbital Contributions[a]

terms	^{2h}K(CH)		^{3h}K(CN)		^{1h}K(OH)		^{2h}K(ON)		^{1}K(NH)		^{1}K(CO)	
FC(σ(NH))	−0.1		1.6	*0.1*	−1.6	*−1.2*	19.0	*14.4*	114.1	*112.8*	−0.8	*−0.1*
		−0.1		*0.1*		*−3.6*		*33.0*		*110.0*		*−0.3*
FC(σ(CO))			1.0	*0.1*	−0.1	*−0.1*	−4.4	*−2.0*	−0.1		318.7	*311.3*
		0.1		*0.2*		*−0.3*		*−3.8*				*312.1*
FC(lp1(O))			0.3		0.5	*−0.3*	15.3	*−6.9*	−0.1		−66.8	*- 55.0*
						−0.8		*−11.1*		*−0.1*		*−52.8*
FC(lp2(O))			0.2		0.6	*1.2*	13.2	*26.1*	−0.1	*−0.5*	−58.2	*−66.2*
		0.1		*0.1*		*5.0*		*48.2*		*−1.4*		*−66.6*
FC(ob)			−1.0	*−0.1*			−7.2	*−5.4*	−14.0	*−13.8*	−53.0	*−50.6*
FC(σ(NH),σ(CO))	−0.3		2.6	*−0.5*	1.1	*0.4*	−11.9	*−4.9*			−0.6	*−0.3*
FC(σ(NH),lp1(O))			0.3		−1.9	*1.0*	21.5	*−13.1*			−0.5	*−0.1*
FC(σ(NH),lp2(O))			0.3		−1.8	*−3.5*	19.4	*40.9*		*0.1*	−0.4	*−0.4*
FC(lp1(O),lp2(O))			−0.2		−0.4	*−0.3*	−8.4	*−5.3*		*−0.1*	34.8	*32.9*
FC(σ(CO),lp1(O))			0.4			*0.1*	0.3	*2.2*			−77.3	*−79.6*
FC(σ(CO),lp2(O))			0.4	*−0.2*	0.0	*−0.1*	0.5	*1.6*			−75.2	*−74.1*
FC(ob,ob)			−2.0	*0.2*	−0.3	*−0.2*	−14.2	*−10.7*	−19.8	*−19.4*	−11.1	*−10.1*
FC(one)	−0.1		2.1	*0.1*	−0.6	*−0.4*	35.7	*26.3*	99.8	*98.4*	140.0	*139.3*
FC(two)	−0.3		1.8	*−0.6*	−3.3	*−2.6*	7.3	*7.5*	−19.7	*−19.3*	−130.3	*−131.5*
FC(total)	−0.4		3.9	*−0.4*	−3.9	*−2.9*	43.0	*33.8*	80.1	*79.1*	9.7	*7.9*
FC(dimer)	−0.4		3.2	*−0.4*	4.1	*−3.0*	36.1	*26.0*	74.9	*74.0*	−38.0	*−39.9*
		0.1		−0.8		−6.1		60.6		72.8		−38.9
PSO(one)	0.1	*−0.1*	0.1		−0.6	*−0.5*	−0.3	*−0.3*	0.5	*0.5*	−14.3	*−14.7*
PSO(two)			0.1		−0.2	*−0.1*	−0.1	*−0.1*	0.1	*0.1*	−14.6	*−14.6*
PSO(total)	0.1	*−0.1*	0.2		−0.8	*−0.6*	−0.4	*−0.4*	0.6	*0.6*	−28.9	*−29.3*
PSO(dimer)	0.2	*−0.1*	0.2		−0.8	*−0.6*	−0.6	*−0.8*	1.2	*1.1*	32.8	*−33.3*
K(total)	−0.2	*−0.9*	4.0	*−0.8*	−4.5	*−2.2*	42.9	*34.4*	80.2	*79.4*	−22.8	*−34.0*
K(dimer)	−0.2	*−0.1*	3.5	*−0.4*	−4.4	*−3.0*	35.8	*25.7*	76.5	*75.6*	−66.9	*−69.3*
		−0.1		*−0.9*		−6.3		60.2		74.0		−67.3

[a] All contributions and SSCCs in SI units. Values in normal print correspond to $\beta = 180$, and those in italics to $\beta = 120°$. The second line of the one-orbital terms gives values calculated at R(O,H) = 1.6 Å and $\beta = 120°$. Orbital contributions smaller than |0.05| SI units have been omitted. Abbreviations FC(one) and FC(two) denote the sum of all one-orbital and two-orbital contributions. The symbol ob (other bonds) denotes contributions from bonds not explicitly considered. FC(dimer) gives the true value for the formamide dimer. The difference FC(total) − FC(dimer) indicates that remote bonds in the monomer not considered in the analysis also contribute (see text).

Can one use them to describe H-bonding and distinguish between covalent and electrostatic H-bonding?

(4) Are there specific steric effects that change the character of H-bonding and are these steric effects reflected by the SSCCs across the HB?

(5) What is the experimental relevance of our analysis?

In Table 1, the calculated SSCCs across the HB of the formamide dimer in its equilibrium geometry are listed together with their one- and two-orbital contributions. On first sight, there is little relationship with the SSCCs of the model system (H_2·H_2) with regard to either sign or magnitude. However, a relationship will be reinstalled if one considers just the steric exchange contribution $K(\sigma(\text{N1H2}),\sigma(\text{O3C4}))$, which is the equivalent to the dominating contribution $K(\sigma(\text{H1H2}),\sigma(\text{H3H4}))$ of the model system. According to the data of Table 1, the signs of these contributions (1−3 contributions, negative; 2−3 and 1−4 contributions, positive) are the same as in the model system although the magnitudes are quite different. The different order of magnitudes results from the fact that zeroth-order LMO(NH) has one, but the corresponding LMOσ(C− O) has two nodal surfaces (the π(C═O) contributes only passively but not actively to the FC term in the planar form of the dimer). The corresponding first-order LMOs have two and three nodal surfaces. The C nucleus will get a small spin density if the perturbation is at H2, and accordingly, a small negative FC(σ-(NH),σ(CO)) contribution results. Hence, inspection of the FC spin density distribution in connection with zeroth- and first-order LMOs quickly explains the relative magnitude of the two-orbital terms, corresponding to the first model system H_2·H_2.

The different signs and magnitudes of the total FC terms (and by this also of the total K values) are a direct result of the participation of the two electron lone pairs at O, which can have a strong effect on the SSCC. Investigation of simple model compounds containing just σ-bonds reveals that the one-bond SSCCs is dominated by the FC term and this in turn by a large, positive bond orbital contribution. Other bonds involving the coupling nuclei lead to smaller, negative contributions (see Scheme 2). If one of the coupling nuclei belongs to a heteroatom with a lone pair, the latter will lead to large, negative one-orbital (Scheme 2) and two-orbital contributions, which can turn around the sign of the FC term and the SSCC. These observations are also relevant for the following discussion of the spin−spin coupling mechanism across a HB. This discussion will consider reduced SSCCs K, which depend just on the electronic structure and thus make a comparison of SSCCs involving different pairs of nuclei possible.

Coupling Constants ^{3h}K(CN) and ^{2h}K(CH). We start with those SSCCs, which both have a chance to be measured, either directly or by an enrichment of ^{15}N in the target molecule. Indeed, all the SSCC information on H-bonding in proteins results from the measurement of the ^{3h}K(CN) constants.[9−17] As shown in Table 1, both ^{3h}K(CN) and ^{2h}K(CH) have the signs to be expected (^{3h}K(CN) > 0; ^{2h}K(CH) < 0), but the magnitude of the 1,3-SSCC is considerably smaller than that of the 1,4-SSCC. The latter decreases with decreasing angle β(COH) and becomes even negative for β close to 120°. The orbital analysis reveals that ^{3h}K(CN) is basically determined by three FC terms at 180: (a) the positive (σ(CO),σ(NH)) steric repulsion term (2.6 SI units), (b) the positive one-orbital term σ(NH) (1.6 SI units), and (c) the positive one-orbital term σ(CO) (1.0 SI units, Table 1). There are no significant active lp contributions because this would require that the O lone pairs possess nonnegligible coefficients at both the C and the N nucleus, which is not

TABLE 2: Active and Passive lp1 and lp2 Orbital Contributions[a]

β	orbital	mode	^{2h}K(CH)	^{3h}K(CN)	^{1h}K(OH)	^{2h}K(ON)	^{1}K(NH)	^{1}K(CO)
180°	lp1	active	0	0.4	−2.4	5.7	0	−51.3
		passive	0	−1.1	0.5	12.3	0	−71.1
		a + p	0	−0.7	−1.9	18.0	0	−122.4
180°	lp2	active	0	0.7	−1.6	16.9	−0.1	−73.5
		passive	0	−0.3	−0.1	−3.1	0	−8.4
		a + p	0	0.4	−1.7	13.8	−0.1	−81.9
180°	lp1 + lp2	active	0	1.1	−4.0	22.6	−0.1	−124.8
		passive	0	0.2	0.9	19.3	0	−124.0
		a + p	0	1.3	−3.1	41.9	−0.1	−248.8
120°	lp1	active	0	0	0.8	−12.2	−0.1	−22.2
		passive	0	−0.1		−6.4	0	−63.2
		a + p	0	−0.1		−18.6	−0.1	−85.4
120°	lp2	active	0	−0.2	−2.7	48.8	−0.5	−114.9
		passive	0	−0.3		−10.7	0.1	−4.6
		a + p	0	−0.5		38.1	−0.4	−119.5
120°	lp1 + lp2	active	0	−0.2	−1.9	36.6	−0.6	−137.1
		passive	0	−0.3	−0.1	−9.5	0.1	−110.4
		a + p	0	−0.5	−2.0	27.1	−0.5	−247.5

[a] All contributions and SSCCs in SI units. Angle β is the COH angle (see Scheme 1). a + p denotes the sum of active and passive contribution. Note that the active contributions involve all one- and two-orbital effects into which the lp orbital is involved, i.e., also those not listed in Table 1. In the case of ^{1h}K(OH), not all passive contributions were calculated.

possible. There is no important active contribution from the covalent coupling mechanism (involving lp delocalization through the space between O and H atom) for SSCC ^{3h}K(CN), which is confirmed when the angle β decreases to 120°: The active lp contributions become smaller rather than larger despite the increasing overlap between lp(O) and σ(NH).

There is, however, a passive FC(lp) contribution, which in the 120° form is −0.3 SI units (Table 2) and which is dominated by the lp2 orbital. The passive contribution in the 180° form (0.2 SI units, Table 2) is relatively small compared to ^{3h}FC(CN) = 3.2 SI units. Repolarization should dominate the passive lp contribution in the linear form, delocalization in the 120° form. Hence, in the 120° form, there is some weak covalent character of the HB that leads to a change in ^{3h}FC(CN) by just −0.3 SI units, which in view of the small magnitude of ^{3h}FC(CN) (−0.4 SI units, Table 1) could be considered as being decisive for the coupling mechanism. This interpretation, however, excludes the fact that in the bent form of the dimer there are also active orbital contributions, which could be considered as being decisive (FC(σ(CO),σ(NH)) = −0.5; FC(σ(CO),lp2(O)) = −0.2 SI units; Table 1).

As in the case of the 1,4-SSCC in H_2·H_2, the one-orbital contributions are positive. Their magnitude depends on the degree of extra-bond polarization caused by the second formamide molecule. This effect is largest in the linear arrangement because both the CO bond, the sum of the lp, and the NH bond dipole moments lead to a strong interaction. These electrostatic interactions decrease in the bent form (β = 120°) as does the steric exchange term between the NH and the CO σ-bond. At 120°, the latter term becomes even slightly negative. We conclude that the SSCC ^{3h}K(CN) depends on both the electric field effect and steric exchange repulsion between the NH and the CO bond. Both effects decrease for a bending to β = 120°. There is a covalent coupling mechanism as reflected by the passive lp contributions (Table 2), which are larger than the active ones. This, however, does not imply that the covalent mechanism is larger that the electric field effect or steric repulsion.

The magnitude of the 1,3-SSCC ^{2h}K(CH) is already rather small (−0.2 SI units) in the linear arrangement and vanishes almost completely in the bent arrangements. This is mainly due to the fact that zeroth-order and/or first-order σ(CO) and σ(NH) orbitals have small coefficients at either H nucleus and/or C nucleus. If the H atom would possess an electron lp as the O atom does, this would be different, as we will see in the following.

Coupling Constants ^{2h}K(ON) and ^{1h}K(OH). Although both SSCCs have little chance to be detected, they provide valuable information for a quantum chemical investigation of H-bonding. The 2,3-SSCC ^{1h}K(OH) would be positive (the two-orbital term (σ(CO),σ(NH)) is 1.1 SI units); if not, the steric exchange terms between lone pair lp1 (or lp2) and the NH bond pair add negative contributions of about −2 SI units each. The result is (adding a one orbital term of −1.6 SI unit for the NH bond orbital, Table 1) a value of −4.1 for the FC term and −4.4 SI units for the total SSCC eventuates.

The spin−spin coupling mechanism for ^{1h}K(OH) can be viewed as a transition from the 2,3 coupling in the H_2 dimer (characterized by a steric exchange interactions) to a covalent coupling mechanism found for ^{1}K(OH) in water. LMO lp2 takes over the role of a bonding orbital when β decreases to 120° and R(O,H) becomes shorter. The lp2(O) contribution increases in this case and becomes 5.0 SI units for R(O,H) = 1.6 (Å) (Table 1), which reflects significant delocalization of lp2(O) into the σ*(NH) orbital, thus enhancing the spin density at the H nucleus. Thus, the lp2(O) orbital contribution is an indicator for a covalent contribution to the coupling mechanism. In the total SSCC ^{1h}K(OH), it is, however, outweighed by the negative σ(NH), σ(CO), lp1(O), and steric exchange contributions, which increase in magnitude with decreasing distance R(O,H). The signs of the various orbital contributions can be easily verified by analyzing the FC spin density distribution or alternatively the extended Dirac vector models developed recently.[32] The lp and NH contributions extend the direct coupling path by one electron pair, thus leading to a negative contribution (see Scheme 2).

The SSCC ^{2h}K(ON) is the most interesting coupling constant across the H-bond. It is the result of six one-orbital and twelve two-orbital contributions with magnitudes larger than one SI unit. The (σ(CO),σ(NH)) term is −11.9 SI units, indicating strong steric exchange repulsion at a distance of 1.9 Å. However, even stronger steric exchange terms result from the two lp orbitals at O. The terms (lp1,σ(NH)) and (lp2,σ(NH)) are 21.5 and 19.4 SI units, respectively, where again the change in sign can be considered as an extension of the coupling path via an "external electron pair", i.e., an electron pair not participating

SCHEME 3

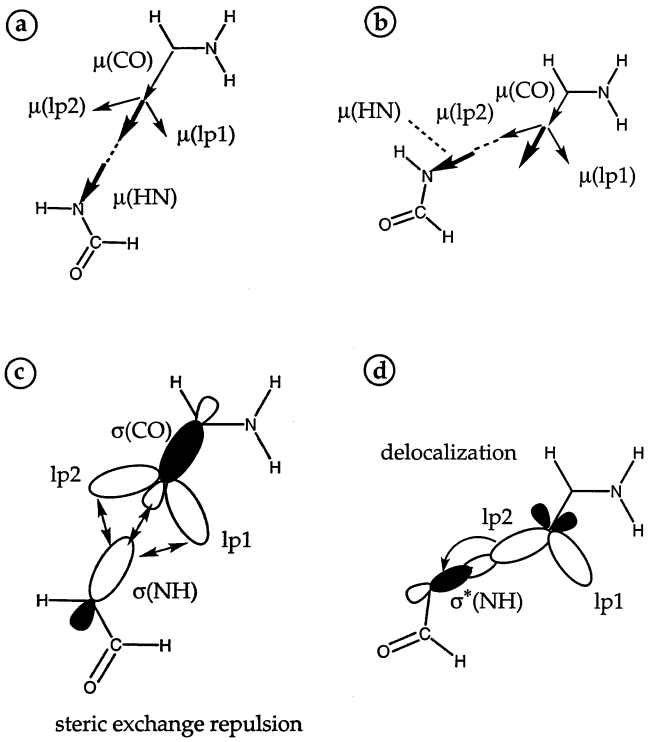

in the direct coupling path from the O to the H and then to the N nucleus. The (lp1,lp2) steric exchange term is −8.4 SI units. The sum of all two orbital terms is 7.3 SI units and it is clearly smaller than the sum of the one-orbital contributions (35.7 SI units).

The one-orbital contributions (σ(NH), lp1, and lp2 (19.0, 15.2, and 13.1 SI units), Table 1) are responsible for the large positive one-orbital FC term, which dominates the total ^{2h}K(ON) value. This could reflect both repolarization (caused by the electric field effect) and delocalization of the electron pairs involved (in the sense of covalent contributions). In view of the orbital energies, delocalization of the NH bond electron pair into the σ^*(CO) orbital cannot make a large contribution, which means that the relatively large NH contribution is mainly due to repolarization of the NH bond density caused by the electric field associated with the second formamide molecule.

This analysis is supported by the geometrical dependence of SSCC ^{2h}K(ON). In the linear arrangement of the HB, charge−charge and dipole−dipole interactions are at their maximum (Scheme 3a,b). For the delocalization of the lp electrons into the σ^*(NH) orbital the overlap is not optimal because of a 60° deviation of the lp orbitals from the NH bond axis (Scheme 3c). Nevertheless, there is a charge transfer of 0.014 electron into the σ^*(NH) orbital, which can be verified by a BSSE-corrected NBO (or Mulliken) analysis of the charge distribution obtained with the basis set used for the SSCC calculations. If the angle β is decreased to 120°, the overlap increases to a maximum and delocalization is facilitated (Scheme 3d), as is reflected by an increase of the charge transfer from 0.014 to 0.025 electron. The lp2 one-orbital contribution increases by almost 13 SI units from 13.2 to 26.1 SI units (Table 1). The lp1 term decreases by 22 SI units from +15.2 to −6.7 SI units, indicating that this electron pair takes now the role of an external pair, which extends the coupling path and leads therefore to a sign inversion (note that one- and two-orbital terms do not necessarily have the same sign). The covalent contribution has doubled in the 120° form, as reflected by the charge-transfer values and the lp2(O) contribution, which again seems to be a suitable indicator for covalent character.

For the purpose of testing this hypothesis, we calculated besides the active also the passive contributions of the lp orbitals (Table 2). Orbital lp2 leads in the linear arrangement of the formamide molecules to a relatively small passive contribution of −3.1 SI units, which increases in magnitude to −10.7 SI units in the bent arrangement (Table 2). The effect is stronger when the passive contribution of both lp orbitals is considered at the same time. In this case, there are three major coupling paths: (a) σ(CO,active) → lp1(O,passive) → σ(NH,active); (b) σ(CO,active) → lp2(O,passive) → σ(NH,active); (c) σ(CO,active) → lp1(O,passive) → lp2(O,passive) → σ(NH,active) or σ(CO,active) → lp2(O,passive) → lp1(O,passive) → σ(NH,active). Because of path c, the passive (and active) lp orbital contributions are not additive (Table 2): The passive orbital contributions of lp1 + lp2 decrease from +19.3 to −9.5 SI units. Inspection of the virtual orbitals reveals that in the linear arrangement repolarization and the electric field effect dominate whereas in the bent form the covalent (delocalization) effect also plays a role. The decrease in the passive FC(1p) contributions can be associated with an increasing importance of a covalent coupling mechanism in line with the observations made for active orbital contributions.

Further confirmation for the role of the covalent effect is obtained by decreasing the distance R(O,H) to 1.6 Å for β = 120°. The charge transfer from the first formamide molecule (acting with its C═O group) to the second (acting with its NH group) increases from 0.025 to 0.054 electron. A similarly strong increase is calculated for the lp2(O) orbital contribution (from 26.1 to 48.2 SI units, Table 1) confirming that charge transfer and lp2(O) contribution are useful indicators for the covalent character of the HB.

Coupling Constants ^1K(NH) and ^1K(CO). These SSCCs are indirectly affected by H-bonding because both NH and CO lengths change with increasing strength of the HB. SSCC ^1K(NH) can be measured, and therefore, it should be analyzed first. Its FC term is positive and dominates the value of the coupling constant. The FC term in turn is dominated by the large NH one-orbital contribution (114.1 SI units, Table 1), which is a result of the electronegativity of N and the large contact spin density at the N nucleus.[33] Other bond contributions (NH2, NC, and the corresponding steric exchange terms such as (σ(NH),σ(NH2)) or (σ(NH),σ(NC)) add negative correction terms to the one-orbital sum. A change in β to 120° leaves these terms unaffected and decreases only the NH one-orbital contribution by 1.4 SI units. This is a result of a weakening of the electric field effect (compare dipole moment directions in Scheme 3a,b).

The J-**OC**-PSP analysis makes it possible to clarify how the second formamide molecule influences the SSCCs ^1K(NH) and ^1K(CO) in the first molecule. For this purpose, all orbital contributions of the second molecule are dropped so that just the effect of the change in the total density (wave function) when converting the monomer to a dimer enters the SSCC. This total density effect accounts for the charge redistribution in the monomer and the charge transfer from one monomer to the other. According to the charge-transfer data discussed above the covalent effect is between 4 and 6%.[51] Hence, the total density effect is dominated by the electric effect in the case of the dimer: The charges of the second monomer generate an electric field, which leads to a charge polarization of the first monomer. In this way, the SSCC ^1K(NH) of the monomer (71.5 SI units, Table 3) increases by 3.5−75.0 SI units.

TABLE 3: Influence of a Second Formamide Molecule on the SSCCs ^1K(NH) and ^1K(CO)[a]

	^{1}FC		^{1}PSO	
terms	^1K(NH)	^1K(CO)	^1K(NH)	^1K(CO)
monomer	71.5	−45.4	1.9	−33.7
dimer, wave function effect	75.0	−35.1	1.3	−32.6
total	80.1	9.7	0.6	−28.9
dimer (full)	74.9	−38.0	1.2	−32.8

[a] All contributions and SSCCs in SI units. Dimer, wave function effects means that the wave functions of the dimer has been calculated; however, only the orbitals contributions of the monomer have been calculated for the FC and PSO term. Total corresponds to the total of Table 1; i.e., it gives the sum of all orbital contributions listed in Table 1. Dimer (full) gives the correct value for FC and PSO term calculated for the dimer.

The electric field effect can be demonstrated for the SSCC ^1K(NH) by mimicking the second formamide molecule by a collection of point charges determined from the NBO analysis[52] of the dimer and positioned at the appropriate locations of the nuclei of the second formamide molecule. In this way, all other effects are excluded. Switching on the electric field effect stepwise by increasing the charges from zero to their actual values leads to a linear increase of both ^1FC(NH) and ^1K(NH) (decrease of ^1J(NH)), as shown in Figure 7a. The electric field effect is larger the shorter R is and the closer β is to 180°. The actual SSCC values ^1J(NH) observed in the dimer for a given distance R(O,H) between 1.9 and 2.2 Å correspond to a charge coefficient of about 0.88 (Figure 7a), reflecting the fact that the real electric field generated by a second formamide molecule results from a continuous charge distribution rather than from point charges, which exaggerate the strength of the electric field. For the same reason it is misleading to represent the second formamide just by one or two point charges associated with the NH group. This strongly exaggerates the influence of the electric field on the SSCC ^1K(NH).

The electron density changes in the first formamide molecules caused by the electric field of the second molecule are shown in Figure 8a,b in the form of electron density difference distributions ρ(monomer + charges) − ρ(monomer). Solid (dashed) contour lines indicate those regions where due to the electric field effect the density of the monomer is increased (decreased). The NH bond density is pushed back onto the N atom (Figure 8a) by the directly opposite negative charge of the O atom, thus leading to an increase of ^1K(NH) via ^{1}FC(NH) and the latter via the σ(NH) orbital contribution. The positive charge directly opposite the C═O bond, draws the density into the space between NH and C═O bond (Figure 8b). Accordingly, the σ(CO) contribution ^{1}FC(CO) becomes smaller whereas the magnitude of the lp2(O) contribution to the through-space SSCCs increases (see Table 1).

The FC term obtained from the total density that embeds the second formamide molecule is almost identical to the total FC term calculated for the dimer when all orbital contributions are included (75.0 versus 74.9 SI units, Table 3), which means that the spin polarization of the electron density of the second molecule is weak or the corresponding contributions cancel each other out. This can be directly checked by inspection of the

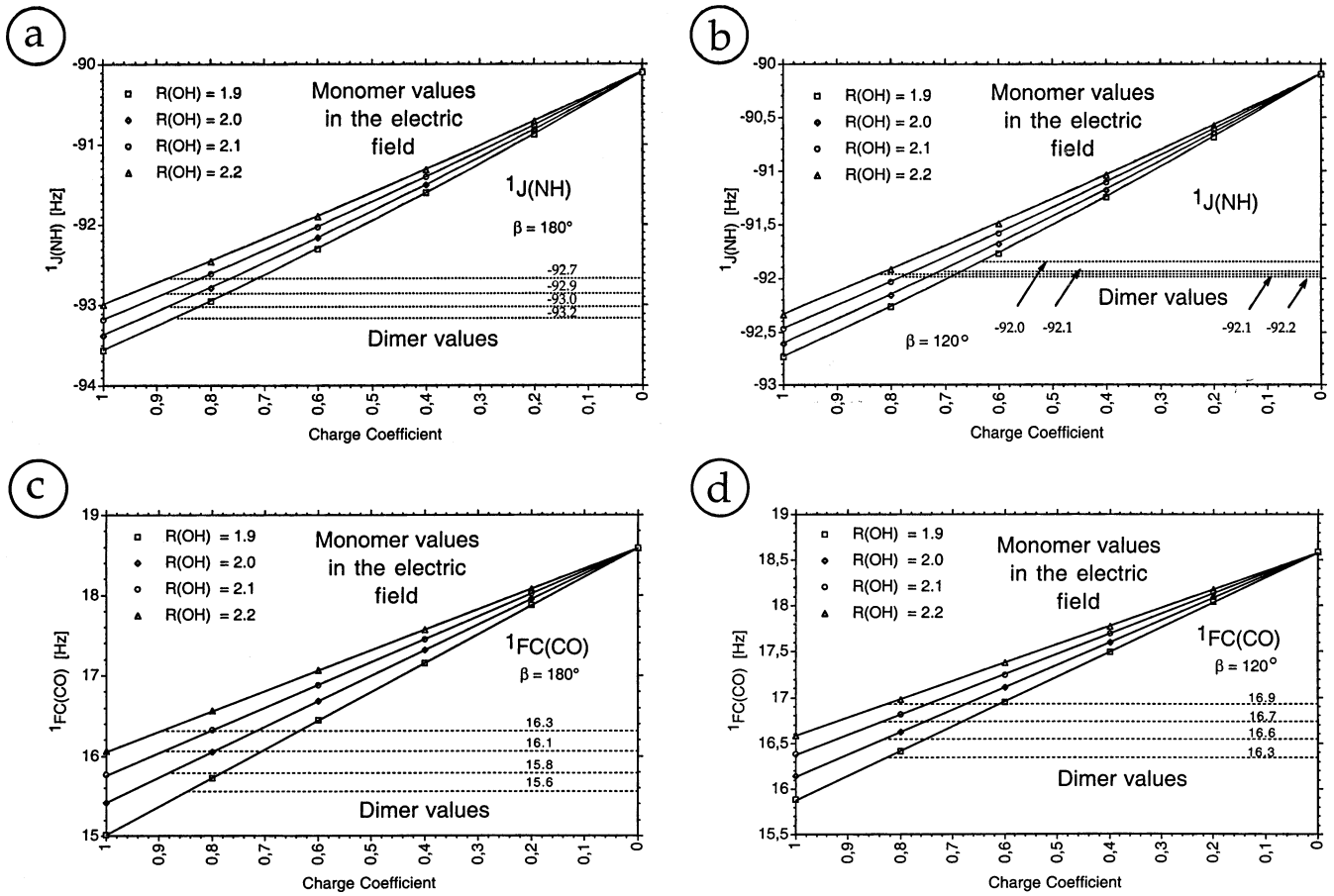

Figure 7. Dependence of ^1J(NH) and ^1J(CO) of the formamide molecule on NBO charges fixed at the positions of the atoms of the partner formamide molecule in the formamide dimer (see Scheme 1a,b). The NBO charges were determined for the dimer and switched on with a charge coefficient increasing from 0 to 1 in the monomer calculations. Horizontal dotted lines give the values of ^1J(NH) and ^1J(CO) in the formamide dimer. All values in hertz. CP-DFT/B3LYP/(11s,7p,2d/5s,1p)[7s,6p,2d/4s,2p] calculations.

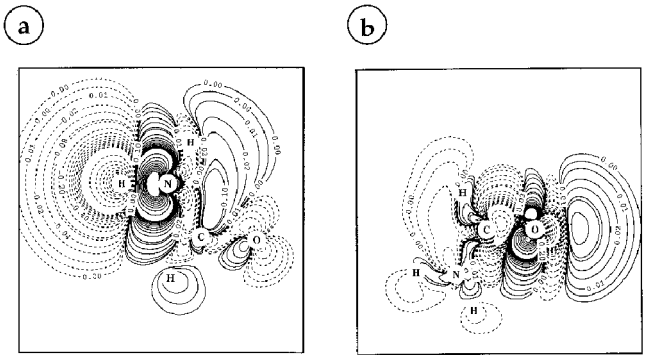

Figure 8. Contour line diagrams of the electron difference density distribution obtained by subtracting the density of the formamide monomer from the density of the monomer under the influence of the atomic NBO charges of a second formamide monomer: (a) NH side of the first formamide molecule; (b) CO side of the second formamide molecule. Solid (dashed) contour lines indicate regions with an increase (decrease) of the density for the perturbed formamide molecule. Charges are opposite to these groups. Contour levels are magnified by 1000 for clarity. B3LYP/(11s,7p,2d/5s,1p)[7s,6p,2d/4s,2p] calculations.

corresponding terms in Table 1. All one- and two-orbital contributions to ^{1}FC(NH) involving the second molecule are negligible. Hence, the electric field effect mediated by the total density is predominantly responsible for the changes in ^{1}FC(NH) caused by dimer formation. This effect is 3.5 Hz and results primarily from the σ(NH) contribution to ^{1}FC(NH). It is responsible for the change in ^1K(NH). The noncontact terms (e.g., the PSO term in Table 3) play a small role.

The electric field effect influencing ^1K(NH) becomes smaller for $\beta = 120°$ because in this direction only one of the electron lone pairs at O interacts with the NH bond (compare Scheme 3a,b). The point charge placed at the position of the O atom of the second formamide molecule exaggerates the electric field effect, which is corrected by a smaller charge coefficient of 0.82 (R = 2.2 Å, Figure 7b). A decrease in the charge coefficient could also imply that another effect becomes important, for example, the steric exchange effect between the NH and the CO bond. Again, investigating the corresponding orbital terms (σ(NH), σ(CO)), (σ(NH),lp1(O)), and (σ(NH),lp2(O)) for both the FC(NH) and the FC(CO) terms (see Table 1) reveals that steric exchange effects between the monomers do not play any role (magnitudes are $\leq$0.6 SI units).

For $\beta = 120°$, the delocalization effect could also become important as donor and acceptor orbital are better aligned. Suitable orbital combination are (1) lp2(O)$-\sigma^*$(NH), (2) σ(CO)$-\sigma^*$(NH), (3) σ(NH)$-\sigma^*$(CO), or (4) σ(NH)$-$Rydberg-(O). Combinations 2$-$4 are unlikely because of inefficient overlap and/or a too large orbital energy difference. Only combination 1 can make a sizable delocalization contribution to FC(NH) and should be reflected by the lp2(O) orbital contribution. This changes, but the changes are too small (Table 1) to serve as suitable indicators for a covalent coupling mechanism. The same is true with regard to the passive role of orbital lp2 (Table 2). The delocalization effect can only become larger for a strongly decreasing R(O,H) (β close to 120°) atypical of HBs in proteins. This would lead to a lengthening of the NH bond because of a transfer of negative charge into the σ^*(NH) orbital (Scheme 3c,d). A longer NH bond implies a decrease of the σ(NH) contribution to ^{1}FC(NH), which is also calculated (110.0 SI units, Table 1).

The SSCC ^1K(CO) has been measured in just a few cases[50] and there is little chance to measure it regularly for proteins. Nevertheless, the CO spin$-$spin coupling mechanism is interesting, as it depends 50% on the FC and to 50% on the PSO + SD interaction (Table 1). The FC contribution is dominated by a large CO one-orbital contribution (319 SI units, Table 1), which is reduced by negative lp contributions ($-$55 and $-$66 SI units; CH, $-$33; CN, $-$17 SI units) and the corresponding negative two-orbital terms ((σ(CO),lp1), $-$79.6; (σ(CO),lp2), 74; (σ(CO),σ(CH)), $-$23.3; (σ(CO),σ(CN)), $-$11.9 SI units; Table 1). In total, a FC term of $-$38 SI units results, which is enlarged in magnitude by the PSO + SD term to $-$66.9 SI units. The largest negative PSO term results from π(CO) ($-$18 SI units).

There are also large passive FC contributions of the lp orbitals being in this case of similar magnitude than the active FC contributions (Table 2). The passive FC contributions establish coupling paths such as (a) σ(CH,active) $\rightarrow$ lp2(O,passive) $\rightarrow$ σ(CO,active), (b) σ(CN,active) $\rightarrow$ lp1(O,passive) $\rightarrow$ σ(CO,active), or (c) σ(CN,active) $\rightarrow$ lp1(O,passive) $\rightarrow$ lp2(O,passive) $\rightarrow$ σ(CO,active), etc., which are obviously rather important for SSCC ^1K(CO) (Table 2).

The wave function effect (Table 3) for ^{1}FC(CO) turns out to be $-$10 SI units (from $-$45.4 to $-$35.1 SI units), which again is predominantly due to the electric field generated by the second molecule. The remaining $-$3 SI units are due to steric exchange terms (from $-$35 to $-$38 SI units, Table 3), thus indicating that the ^{1}FC(CO) term is somewhat more sensitive to the spin polarization of the NH bond of the second molecule. A change in the geometry yielding the bent form with $\beta = 120°$ leads to a change in the FC term by $-$2 SI units, mainly caused by a reduction of the positive σ(CO) contribution (from 319 to 311 SI units, Table 1). This is caused by the change in the electric field (Scheme 3a,b, Figure 7c,d), as discussed above.

For the purpose of analyzing H-bonding, only a subset of orbital contributions has been listed in Table 1. If this is summed up, the SSCC terms FC(total), PSO(total), etc. listed in Tables 1 and 3 will be obtained. Comparison of these values with the final value for the dimer, i.e., FC(dimer), PSO(dimer), etc., indicates whether monomeric terms (i.e., terms not having to do with H-bonding) have been neglected. For example, the large discrepancy of 48.7 SI units between the "total" and the "dimer" value of ^1K(CO) (see Table 3) results form steric exchange terms such as (c(C),lp1(O)) = $-$8.4, (c(C),lp2(O)) = $-$2.5, (c(O),lp1(O)) = $-$27.3 or (c(O),lp2(O)) = $-$14.5 SI units, where c(C) and c(O) denote the core orbitals of C and O, respectively.

5. Conclusions

This work has provided an insight into both the spin$-$spin coupling mechanism across the HB and the nature of H-bonding in a typical situation mimicking that of H-bonding in proteins. Using the H_2 dimer and the formamide dimer as appropriate model systems, a number of conclusions can be drawn from the calculated SSCCs and their decomposition with the help of the J-**OC**-PSP analysis.

(A) Spin$-$Spin Coupling through Space between Protons. (1) Spin$-$spin coupling through-space involving protons is dominated by the FC contribution because spin polarization can bridge larger distances than orbital currents. The FC contributions are mediated by the two-orbital terms describing predominantly steric exchange interactions. At larger distances, there are just weak dispersion interactions that mediate the FC mechanism.

(2) The steric exchange terms lead to an oscillation of the sign of the FC terms and by this also of the J values: ^1J(H2,H3) > 0, ^2J(H1,H3) < 0, ^3J(H1,H4) > 0, and a steady increase of the magnitude of the through-space SSCC from short-range to

long-range, i.e., SSCC ^3J(H1,H4) has the largest value. Sizable values are obtained for R(H2,H3) distances smaller than 2.4 Å in the case of ^3J(H1,H4), smaller than 2 Å in the case of ^2J(H1,H3), and smaller than 1.6 Å in the case of ^1J(H2,H3); i.e., in the latter case spin−spin coupling is only relevant for the situation of strong steric interactions, which lead to bond rearrangements.

(3) The steric exchange terms depend on the spin density of the coupling nuclei, which in turn is a result of the product of zeroth-order and first-order orbital amplitudes at these positions. The analysis shows that the nodal behavior of the zeroth-order orbitals has the strongest impact on sign and magnitude of the SSCC. The nodal behavior of the first-order orbitals is largely predictable once the nucleus to be perturbed has been chosen.

(4) Zeroth-order atomic densities (NBO, Mulliken, etc.) or s-densities at the nucleus are of no, or only indirect, importance for the FC coupling mechanism. The s-densities at the coupling nuclei are not necessarily parallel to the spin densities at these positions. This will have to be considered if simplified models based on the s-character of hybrid orbitals are used to explain the magnitude of the FC term.

(B) Spin−Spin Coupling across the H-Bond. (1) The spin−spin coupling mechanism across the HB in a protein or peptide involves three effects: (a) a dominant electric field effect (electrostatic effect), (b) steric exchange interactions, and (c) a weak covalent effect (transfer of electronic charge).

(2) The electric field effect can be tested (a) by using the wave function of the dimer but excluding all orbital terms from the second molecule in the SSCC calculation, (b) with the use of probe charges for the second monomer when calculating the SSCCs of the first, and (c) by difference density maps calculated for the monomer with and without probe charges. A negative charge opposite to the N−H bond leads to increased polarization of the N−H bond, a larger contact density at the N nucleus, and a stronger FC coupling mechanism, which can be documented for ^1J(NH) in the monomer (the negative SSCC becomes more negative). Similarly, a positive charge opposite to the O═C bond, distorts the O density into the direction of the external charge and in this way decreases the (positive) SSCC ^1J(CO). The electric field effect is reflected by the one-orbital terms. It corresponds to $k \rightarrow k^*$ excitations and leads to a repolarization of the density in the bond affected (increase or decrease in the polarity of the bond).

(3) The steric exchange effect depends on the penetration of tail densities of opposite bonds or electron lone pairs. It decreases exponentially with decreasing overlap (increasing interaction distance or decreasing bending angle β).

(4) The covalent effect results from delocalization contributions to the one-orbital term. Delocalization effects require a high-lying occupied orbital that can efficiently overlap with a low-lying unoccupied orbital prone to accept electronic density. In the H-bonding situation these are the electron lone pair orbital at the heteroatom (e.g., at the O(═C) atom) and the σ^*(XH) MO of the H donor group, i.e., lp(O) $\rightarrow$ σ^*(NH) excitations. Delocalization from σ(NH) to σ^*(CO) is also possible but, because of the much larger orbital energy difference, less effective.

(5) The covalent effect can be transmitted via active and passive orbital contributions. In both cases, the covalent coupling mechanism is that of lp2(O) in the model used. It is most sensitive in the case of the SSCC ^{2h}J(ON), detectable but not as useful because of its relatively small magnitude for SSCCs ^{1h}J(OH) and ^1J(NH). In the case of SSCC ^{3h}J(CN), there is also a significant (compared to the absolute magnitude of the SSCC) passive lp2(O) contribution in the bent arrangement of the formamide molecules leading to a covalent coupling mechanism.

(6) Combining BSSE corrected charge-transfer values with covalent lp2(O) contributions to calculated FC terms, we estimate the covalent character of typical HB in proteins to be not larger than 15%.

(7) The electric field effect is responsible for the angular dependence of the magnitude of the SSCCs across the HB. The magnitude always decreases when the angle β decreases from 180 to 120° (linear to bent) arrangement because of the decrease of the electric field effect as shown in Scheme 3. In a simplified way one can speak of two coupling mechanisms I and II: I is active in the linear form and is dominated by electric field effect and steric exchange repulsion; II includes also a nonnegligible covalent coupling contribution.

(C) Practical Considerations. (1) The through-space spin−spin coupling mechanism active in the H_2 dimer is of relevance when predicting and analyzing proton−proton coupling in half-cage compounds such as **1** or **2**, for which values of 1.5 Hz

J(A,B) = 1.1 Hz J(A,B) = 1.1 Hz

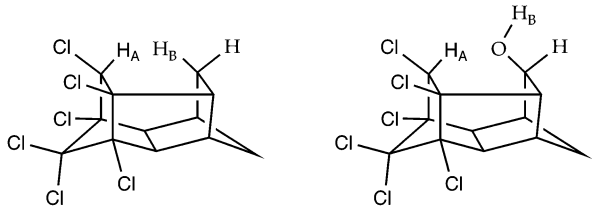

1 **2**

were measured.[53] According to the analysis carried out in this work, the SSCC for **1** should be positive, that for **2** should be negative.

(2) Experimental attempts to measure SSCC ^{2h}J(CH) across a HB will be fruitless because this SSCC will have always rather small values.

(3) The only SSCC across the HB in proteins so far measured is ^{3h}J(CN).[11,12] This SSCC is always rather small in magnitude ($|^{3h}J(\mathrm{CN})| < 1$ Hz) but mostly negative (the reduced SSCC K is positive). The coupling mechanism depends predominantly on the electric field and the steric exchange effects involving σ(NH) and σ(CO). This is the reason why it is relatively easy to relate the values of ^{3h}J(CN) to distance R(O,H) and angle β. For a linear arrangement ($\beta = 180°$ the largest electric field effect can be expected thus yielding in this situation the largest negative ^{3h}J(CN) values. Small negative or even positive ^{3h}J(CN) values indicate bending of the COH angle β and an admixture of a covalent coupling mechanism. Especially revealing in this connection is the partitioning of the various orbital contributions in active and passive parts. In parallel work we have extensively investigated SSCCs ^{3h}J(CN) of the protein ubiquitin.[54] The trends observed in this work are also found in the measured and calculated values of ubiquitin.

(4) Even if it is not possible to measure the SSCC across the HB, valuable information on the latter can be drawn from the measured SSCC ^1J(NH). This SSCC depends largely on the electric field effect of the second monomer, and therefore, it directly reflects the distance and angular dependence of this effect. SSCC ^1J(NH) is negative and becomes more negative upon HB formation where this change is largest for a linear approach C═O···HN ($\beta = 180°$). For smaller values β, ^1J(NH) becomes more positive. These trends have been calculated to describe H-bonding in the protein ubiquitin.[54]

(5) Although SSCCs ^{1h}J(OH) and ^{2h}J(ON) across the HB cannot be measured at the moment, they offer insight in the covalent character of the HB via their lp(O) contributions to the FC term, where the effects are larger for ^{2h}J(ON). Therefore, the latter SSCC is best suited to assess the covalent character of a coupling mechanism across the HB with the help of quantum chemical calculations. In this connection the J-**OC**-PSP method is an excellent tool to determine these effects.

(6) The zeroth-order density is not changed by spin−spin coupling. Hence, any conclusion concerning the nature of H-bonding must be valid for both the zeroth-order and first-order density distribution. Applying the Cremer−Kraka criterion of covalent bonding,[55] there is clearly no covalent bond between H(N) and O(═C) atoms, as tested in this work and by other authors.[21] The interactions are dominantly electrostatic with some minor covalent contributions (less than 15% considering a range of typical *R* distances), which increase of course for significantly smaller *R* distances.

(7) In this work cooperative effects strengthening (or weakening) H-bonding in a protein are not considered because their modeling requires more sophisticated models than that of a formamide dimer. In our investigation of the protein ubiquitin, cooperative effects influencing the geometry of HB were found and thus also indirectly affect the magnitude of the across-HB SSCCs. Other than these geometrical effects were not observed.[54]

Acknowledgment. This work was supported by the Swedish Research Council (Vetenskapsrådet). Calculations were done on the supercomputers of the Nationellt Superdatorcentrum (NSC), Linköping, Sweden. D.C. thanks the NSC for a generous allotment of computer time.

References and Notes

(1) (a) *Hydrogen Bonding in Biological Structures*; Jeffrey, G. A., Saenger, W., Eds.; Springer: Berlin, 1991. (b) Jeffrey, G. A. *An Introduction to Hydrogen Bond*; Oxford University Press: New York, 1997.

(2) Scheiner, S. *Hydrogen Bonding*; Oxford University Press: New York, 1997.

(3) Desiraju, G. R.; Steiner, T. *The Weak Hydrogen Bond*; Oxford University Press: New York, 1999.

(4) (a) Chang, H.-C.; Lee, K. M.; Jaing, J.-C.; Lin, M.-S.; Lin, I. J. B.; Lin, S. H. *J. Chem. Phys. A* **2002**, *117*, 1723. (b) Lindeman, S. V.; Kosynkin, D.; Kochi, J. K. *J. Am. Chem. Soc.* **1998**, *120*, 13268. (c) Hunter, C. A. *Chem. Soc. Rev.* **1994**, *23*, 101. (d) Hunter, C. A.; Sanders, J. K. M. *J. Am. Chem. Soc.* **1990**, *112*, 5525. (e) Askew, B.; Ballester, P.; Buhr, C.; Jeong, K. S.; Jones, S.; Parris, K.; Williams, K.; Rebek, J. *J. Am. Chem. Soc.* **1989**, *111*, 1082. (f) Zimmerman, S. C.; VanZyl, C. M.; Hamilton, G. S. *J. Am. Chem. Soc.* **1989**, *111*, 1373. (g) Shepodd, T. J.; Petti, M. A.; Dougherty, D. *J. Am. Chem. Soc.* **1988**, *110*, 1983. (h) Rebek, J. *Angew. Chem., Int. Ed. Engl.* **1990**, *29*, 245. (i) Diedrich, F. *Angew. Chem., Int. Ed. Engl.* **1988**, *27*, 362.

(5) (a) Kim, K. S.; Tarakeshwar, P.; Lee, J. Y. *Chem. Rev.* **2000**, *100*, 4145. (b) Brutschy, B. *Chem. Rev.* **2000**, *100*, 3891.

(6) (a) Krimm, S.; Kuroiwa, K. *Biopolymers* **1968**, *6*, 401. (b) Krimm, S. *Nature* **1966**, *212*, 1482. (c) Scheiner, S.; Kar, T.; Gu, Y. *J. Biol. Chem.* **2001**, *276*, 9832. (d) Burely, S. K.; Petsko, G. A. *Science* **1985**, *229*, 23. (e) Blundell, T.; Singh, J.; Thornton, J.; Burley, S. K.; Petsko, G. A. *Science* **1986**, *234*, 1005. (f) Burely, S. K.; Petsko, G. A. *J. Am. Chem. Soc.* **1986**, *108*, 7995. (g) Brandl, M.; Weiss, M. S.; Jabs, A.; Suhnel, J.; Hilgenfeld, R. J. *Mol. Biol.* **2001**, *307*, 357. (h) Toth, G.; Murphy, R. F.; Lovas, S. *Protein Eng.* **2001**, *14*, 543.

(7) Blatchford, M. A.; Raveendran, P.; Wallen, S. L. *J. Am. Chem. Soc.* **2002**, *124*, 14818.

(8) Desiraju, G. R. *Acc. Chem. Res.* **1996**, *29*, 441.

(9) Dingley, A. J.; Grezeseik, S. *J. Am. Chem. Soc.* **1998**, *120*, 8293.

(10) Pervushin, K.; Ono, A.; Fernández, C.; Szyperski, T.; Kainosho, M.; Wüthrich, K. *Proc. Natl. Acad. Sci. U.S.A* **1999**, *121*, 6019.

(11) Cordier, F.; Grezeseik, S. *J. Am. Chem. Soc.* **1999**, *121*, 1601.

(12) Cornilescu, G.; Hu, J.-S.; Bax, A. *J. Am. Chem. Soc.* **1999**, *121*, 2949.

(13) Cornilescu, G.; Ramirez, B. E.; Frank, M. K.; Clore, G. M.; Gronenborn, A. M.; Bax, A. *J. Am. Chem. Soc.* **1999**, *121*, 6275.

(14) Cordier, F.; Rogowski, M. Grzesiek, S.; Bax, A. *J. Magn. Reson.* **1999**, *140*, 510.

(15) (a) Wang, Y.-X.; Jacob, J.; Cordier, F.; Wingfield, P.; Stahl, S. J.; Lee Huang, S.; Torchia, D.; Grezeseik, S.; Bax, A. *J. Biomol. NMR* **1999**, *14*, 181. (b) Lohr, F.; Mayhew, S. G.; Ruterjans, H. *J. Am. Chem. Soc.* **2000**, *122*, 9289.

(16) Dingley, A. J.; Masse, J. E.; Feigon, J.; Grezeseik, S. *J. Biomol. NMR* **2000**, *16*, 279

(17) Sychrovsky, V.; Vacek, J.; Hobza, P.; Zidek, L.; Sklenar, V.; Cremer, D. *J. Phys. Chem. B* **2002**, *106*, 10242.

(18) (a) Scheurer, C.; Brüschweiler, R. *J. Am. Chem. Soc.* **1999**, *121*, 8661. (b) Case, A.; Scheurer, C.; Brschweiler, R. *J. Am. Chem. Soc.* **2000**, *122*, 10390.

(19) Pecul, M.; Sadlej, J. *Chem. Phys. Lett.* **1999**, *308*, 486.

(20) Benedict, H.; Shenderovich, I. G.; Malkina, O. L.; Malkin, V. G.; Denisov, G. S.; Golubev, N. S.; Limbach, H. H. *J. Am. Chem. Soc.* **2000**, *122*, 1979.

(21) Arnold, W. D.; Oldfield, E. *J. Am. Chem. Soc.* **2000**, *122*, 12835.

(22) Bagno, A. *Chem. Eur. J.* **2000**, *6*, 2925.

(23) (a) Del Bene, J. E.; Perera, S. A.; Bartlett, R. J. *J. Am. Chem. Soc.* **2000**, *122*, 3560. (b) Del Bene, J. E.; Bartlett, R. J. *J. Am. Chem. Soc.* **2000**, *122*, 10480.

(24) Del Bene, J. E.; Perera, S. A.; Bartlett, R. J. *J. Phys. Chem. A* **2001**, *105*, 930.

(25) Wilkens, S. J.; Westler, W. M.; Weinhold, F.; Markley, J. L. *J. Am. Chem. Soc.* **2002**, *121*, 1601.

(26) Barfield, M. *J. Am. Chem. Soc.* **2002**, *124*, 4158.

(27) Alabugin, I. V.; Mancharan, M.; Peabody, S.; Weinhold, F. *J. Am. Chem. Soc.* **2003**, *125*, 5973.

(28) (a) Cleland, W. W.; Kreevoy, M. M. *Science* **1994**, *264*, 1887. (b) Cleland, W. W.; Kreevoy, M. M. *Science* **1995**, *269*, 104.

(29) Tobin, J. B.; Whitt, S. A.; Cassidy, C. S.; Frey, P. A. *Biochemistry* **1995**, *34*, 6919.

(30) Garcia-Viloca, M.; Gelabert, R.; Gonzales-Lafort, A.; Moreno, M.; Llush, M. J. *J. Phys. Chem. A* **1997**, *101* , 8727.

(31) Schiott, B.; Iversen, B. B.; Madsen, G. K. H.; Bruice, T. C. *J. Am. Chem. Soc.* **1998**, *120*, 12117.

(32) Gräfenstein, J.; Wu, A.; Tuttle, T.; Cremer, D. Submitted for publication.

(33) Wu, A.; Gräfenstein, J.; Cremer, D. *J. Phys. Chem. A* **2003** *107*, 7043.

(34) Wu, A.; Cremer, D. *Phys. Chem. Chem. Phys.*, in press.

(35) Ramsey, N. F. *Phys. Rev.* **1953**, *91*, 303.

(36) Sychrovsky, V.; Gräfenstein, J.; Cremer, D. *J. Chem. Phys.* **2000**, *113*, 3530. See also: (b) Helgaker, T.; Watson, M.; Handy, N. C. *J. Chem. Phys.* **2000**, *113*, 9402.

(37) Boys, S. F. *Rev. Mod. Phys.* **1960**, *32*, 296.

(38) Huber, K. P.; Herzberg, G. *Molecular Spectra and Molecular Structure, IV. Constants of Diatomic Molecules*; Van Nostrand: New York, 1979.

(39) For a recent review, see: Cremer, D. *Encyclopedia of Computational Chemistry*; Schleyer, P. v. R., Allinger, N. L., Clark, T., Gasteiger, J., Kollman, P. A., Schaefer, H. F., III, Schreiner, P. R., Eds.; Wiley: Chichester, 1998; Vol. 3, p 1706. See also: Møller, C.; Plesset, M. S. *Phys. Rev.* **1934**, *46*, 618.

(40) Dunning, T. H., Jr. *J. Chem. Phys.* **1989**, *99*, 107.

(41) Becke, A. D. *J. Chem. Phys.* **1993**, *98*, 5648.

(42) (a) Becke, A. D. *Phys. Rev. A* **1988**, *38*, 3098. (b) Lee, C.; Yang, W.; Parr, R. P. *Phys. Rev. B* **1988**, *37*, 785.

(43) Kutzelnigg, W.; Fleischer, U.; Schindler, M. In *NMR−Basics Principles and Progress*; Springer: Heidelberg, 1990; Vol. 23, p 165.

(44) Berger, S.; Braun, S.; Kalinowski, H.-O. *NMR Spectroscopy of the Non-Metallic Elements*; Wiley: Chichester, U.K., 1997.

(45) Boys, F.; Bernardi, F. *Mol. Phys.* **1970**, *19*, 553.

(46) COLOGNE2003, Kraka. E.; Gräfenstein; J.; Filatov, M.; He, Y.; Gauss, J.; Wu, A.; Polo, V.; Olsson, L.; Konkoli, Z.; He. Z.; Cremer D. Göteborg University, Göteborg, 2003.

(47) (a) Kowalewski, J. *Prog. NMR Spectrosc.* **1977**, *11*, 1. (b) Kowalewski, J. *Annu. Rep. NMR Spectrosc.* **1982**, *12*, 81.

(48) Boykin, D. W. *^{17}O NMR Spectroscopy in Organic Chemistry*; CRC Press: Boca Raton, FL, 1991.

(49) Berger, S.; Braun, S.; Kalinowski, H.-O. *NMR Spectroscopy of the Non-Metallic Elements*; Wiley: Chichester, U.K., 1997.

(50) (a) Kintzinger, J.-P. *Oxygen NMR: Characteristic parameters and applications in NMR-17. Oxygen-17 and Silicon-29*; Diehl, P., Fluck, E., Kosfield, R., Eds.; Sringer Verlag: New York, 1981; p 1. (b) Kintzinger, J.-P. In *Oxygen-17 NMR*; Laszlo, P., Ed.; NMR of Newly Accessible Nuclei, Vol. 2; Academic Press: New York, 1983; Chapter 4.

(51) For the purpose of estimating the magnitude of the covalent effect, we take the H_3^- anion or the allyl anion as a suitable reference. In these

molecules the charge of the terminal atoms is 1.5, as that of the central atom 1 s or π electron. In the system O···H···N the charges should be about 1.60, 1, and 1.4 electrons in view of the electronegativity difference. Hence, a charge transfer of 0.4 electron from lp2(O) into the σ^*(NH) orbital at an appropriate distance R(O,H) should lead to covalent bonding. Using this value as reference one obtains the percentages given in the text. Note that the one-orbital contributions always contain the repolarization effect, thus making an estimate of the covalent effect difficult.

(52) (a) Carpenter J. E.; Weinhold, F. *J. Mol. Struct. (THEOCHEM)* **1988**, *169*, 41. (b) Reed, A. E.; Weinhold, F. *J. Chem. Phys.* **1983**, *78*, 4066. (c) Reed, A. E.; Curtiss, L. A.; Weinhold, F. *Chem. Rev.* **1988**, *88*, 899.

(53) See, e.g.: Marchand, A. P. *Stereochemical Application of NMR studies in Rigid Bicyclic Systems*; VCH: Deerfield Beach, FL, 1982.

(54) Tell, T.; Wu, A.; Kraka, E.; Cremer, D. To be published.

(55) (a) Cremer, D.; Kraka, E. *Angew. Chem., Int. Ed. Engl.* **1984**, *23*, 62. (b) Cremer, D.; Kraka, E. *Croat. Chem. Acta* **1984**, *57*, 1259.